



ELSEVIER

Physics of the Earth and Planetary Interiors 115 (1999) 293–312

PHYSICS
OF THE EARTH
AND PLANETARY
INTERIORS

www.elsevier.com/locate/pepi

Source effects on surface wave group travel times and group velocity maps

Anatoli L. Levshin ^{*}, Michael H. Ritzwoller, Joe S. Resovsky

Department of Physics, University of Colorado at Boulder, Campus Box 390, Boulder, CO 80309, USA

Received 29 January 1999; accepted 9 June 1999

Abstract

In most seismic surface wave studies observed group travel times are interpreted as time delays due entirely to the wave propagation along the wave path, and source effects are considered as negligibly small. This is in contrast with observed phase times where correction for the source phase is generally acknowledged to be mandatory. An important, yet unanswered, question is how neglecting source group time (SGT) in broadband surface wave studies will affect the accuracy of the measured group velocity curves and the tomographic maps constructed from these measurements. We consider here the effect of SGT on group velocity measurements for fundamental Rayleigh waves and report on its dependence on period (10–200 s), source mechanism, and source depth. Varying these parameters strongly affects the magnitude and azimuthal pattern of SGT shifts and we present statistics of certain salient functionals that characterize this dependence. SGT is negligible for periods less than about 75 s and for earthquake shallower than about 25 km. At longer periods and for deeper events, average SGT corrections are greater than 10 s in magnitude, which for continental scale studies translates into group velocity perturbations of 1–2%. We estimate the bias caused by uncorrected SGT in inversions for Rayleigh wave group velocity maps across the Eurasian continent. The largest perturbations to these maps (up to 1–2% for the 50-s period and up to 5% for the 100-s period) are found near the periphery of the continent where ray coverage is poor. From these results, some statistical estimates for adjacent wave paths (clusters), and the fact that SGT corrections display considerable sensitivities to earthquake depths, we conclude that the effects of SGT on group velocity tomographic images may safely be ignored at periods less than about 75 s and for shallow sources. Although such corrections are appreciable at longer periods for events deeper than about 25 km and should in principle be applied, the inherent inaccuracy of present day CMT solutions and group velocity measurements make these corrections practically non-essential for current group velocity tomographic studies. © 1999 Elsevier Science B.V. All rights reserved.

Keywords: Surface waves; Tomography; Seismic source

1. Introduction

Surface wave tomographic studies are commonly based on phase and group velocity dispersion mea-

surements (e.g., Zhang and Tanimoto, 1993; Wu and Levshin, 1994; Trampert and Woodhouse, 1995; Laske and Masters, 1996; Curtis and Woodhouse, 1997; Ekström et al., 1997; Wu et al., 1997; Ritzwoller and Levshin, 1998; Ritzwoller et al., 1998). Two distinct approaches to such measurements are in practice today. The first is based on direct measure-

^{*} Corresponding author. Tel.: +1-303-492-6952; fax: +1-303-492-7935; E-mail: levshin@lemond.colorado.edu

ments of surface wave functionals such as phase and group velocities, particle motion (ellipticity, polarization), and amplitudes as functions of period (e.g., Knopoff, 1972). The second is based on waveform fitting (e.g., Woodhouse and Dziewonski, 1984; Nallet, 1987; Snieder, 1988) in which phase velocity curves, phase velocity maps, or seismic models of the Earth are iteratively improved by comparing synthetic waveforms to observations.

In the first, and more traditional, approach apparent surface wave velocities may be distorted by the effect of the so-called ‘source phase’ (e.g., Knopoff and Schwab, 1968). The source phase is the phase of a complex excitation function produced by convolving the components of the strain tensor carried by a given surface wave and evaluated at the source depth with the elements of the moment tensor. This function is one of several factors that define the surface wave spectrum (e.g., Gilbert, 1976; Aki and Richards, 1980). The nature of this excitation function, and consequently its phase, depends on frequency, source mechanism, depth, and the seismic structure of the medium near to the source. Source phase is an initial phase that introduces a temporal shift in the measurement of a phase time and, hence, a perturbation in phase velocity. We call this shift the ‘source phase time’ (SPT) shift. In addition, there is an associated shift in group time which produces a perturbation in group velocity. ‘Source group time (SGT)’ shift is related to the frequency derivative of source phase. If source phase is nearly frequency-independent, SGT is very small.

It is commonly reported (e.g., Knopoff and Schwab, 1968) that at periods below about 50 s, source phase depends only weakly on frequency and, hence, SGT shifts at these periods are usually neglected in most group velocity studies. This is, in fact, one of the features that commends the use of group velocity measurements over phase velocities at relatively short periods. Group velocity measurements are not as strongly contaminated by source effects and it is believed that group velocity measurements can be made and used without a knowledge of the source mechanism.

In contrast, the need to introduce SPT corrections into phase velocity measurements has long been recognized (e.g., Knopoff and Schwab, 1968; Panza et al., 1973) and is now a part of most processing

routines. If the source mechanism and a regional model of the medium near to the source are known, it is possible to compute the necessary phase corrections and to remove them from phase measurements leaving only perturbations in phase produced during the propagation of the wave. The main difficulty in applying source phase corrections is the inherent inaccuracy of estimates of the source depth and mechanism. This information is commonly taken from global catalogs such as the Harvard Centroid Moment Tensor (CMT) catalog (e.g., Dziewonski et al., 1981). The accuracy of depth and moment tensor estimates presented in such catalogs depends strongly on the magnitude, spatial location, and depth of an event. The relative accuracy of depth estimates is particularly poor for crustal events in coarsely instrumented regions. Muyzert and Snieder (1996) analyzed the effect of uncertainties in source depth and source mechanism on phase velocity corrections and found that this effect is significant, especially for Rayleigh waves.

Although group velocities probably remain somewhat less used than phase velocities, they are commonly utilized in the analysis of small regional events, in seismic verification research (e.g., Stevens and Day, 1985), and, recently, at long periods for the study of the crust and upper mantle (e.g., Ritzwoller and Levshin, 1998). There are several different techniques for obtaining such measurements; all involve direct measurements made on the observed seismogram and use some kind of windowing of the observed signals in the time, frequency, or a time–frequency domains to suppress interference from unwanted signals (e.g., Cara, 1973; Dziewonski et al., 1969; Landisman et al., 1969; Knopoff, 1972; Levshin et al., 1972, 1989, 1992; Russell et al., 1988; Ritzwoller et al., 1995). No a priori model of the medium of propagation is needed for such measurements, and most of these methods do not include any model fitting procedures. Source corrections for group velocity measurements are commonly considered to be negligibly small and have not been applied to observed group velocities in most of related studies. Exceptions are Cara and Hatzfeld (1976) who noted that SGT is zero only for particular source mechanisms and Jimenez et al. (1989) in which the authors analyzed the importance of such corrections in determining selected source mecha-

nisms. Calcagnile et al. (1982) and Vdovin et al. (1999) applied SGT corrections in their structural studies. However, taking into account the growing use of broadband group velocity data in modern surface wave tomographic studies aimed at obtaining detailed and reliable 3D structure of the Earth's lithosphere, we believe that it would be useful to investigate the accuracy of the approach neglecting

SGT corrections. We will limit our discussion to Rayleigh waves, as our calculations have shown that for Love waves the SGT is negligible in the period band (10–200 s) and source depth range (0–200 km). We also ignore here effects caused by the finite duration and finite size of earthquake sources. These effects are usually strongly diminished by using CMT centroid estimates (Dziewonski et al., 1981) as the

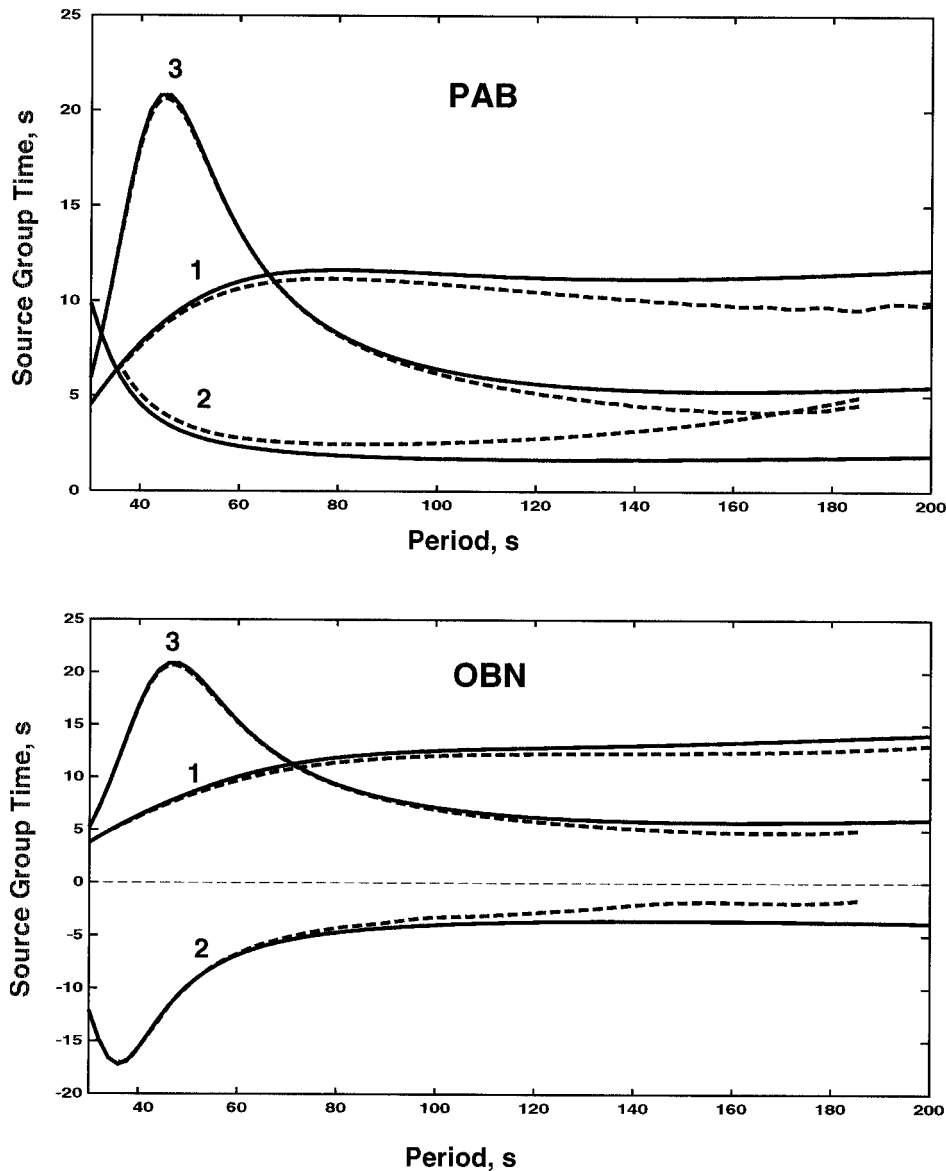


Fig. 1. Comparison of two types of computed SGT curves. Curves of the first type (solid lines) are from the asymptotic formalism in Appendix A. Curves of the second type (dashed lines) are found by the spectral analysis of synthetic seismograms obtained by non-asymptotic normal mode summation. All calculations are performed for three events from the Harvard CMT catalog (1: 1/01/96, Sulawesi; 2: 10/09/96, Cyprus; 3: 10/23/96, Philippines) at two recording stations in Eurasia (OBN and PAB). Differences between asymptotic and non-asymptotic curves are negligibly small (less than 3 s) in all cases.

source time and spatial coordinates instead of hypocenter determinations. The estimates of possible bias in group velocity tomographic maps introduced by errors in event locations were presented earlier in the work of Ritzwoller and Levshin (1998).

The goal of this paper is to evaluate the possible effects of SGT on group velocity measurements and tomographic maps constructed by inverting Rayleigh wave group velocity data. We will estimate the range of periods and source depths for which corrections due to SGT are negligible or practically non-essential in comparison with the inherent inaccuracy of the group velocity measurements and CMT solutions.

2. Theoretical background

The asymptotic formalisms defining surface wave waveforms and spectra in laterally homogeneous media and smoothly laterally inhomogeneous media are summarized briefly in Appendix A. The expressions for the source phase and the SGT shift for a given surface mode in a laterally homogeneous half-space are given by formulas (A16, A17, A22, A23). In the case of a smooth laterally inhomogeneous medium, these functions are described by similar formulas.

To estimate the validity of these asymptotic formulas, we computed a set of theoretical seismograms of the fundamental Rayleigh wave for several events from the Harvard CMT catalog at several stations of the Global Seismic Network. We used a non-asymptotic normal mode representation of the seismic wave field in a spherically symmetric isotropic earth model (Gilbert and Dziewonski, 1975). After converting seismograms to the spectral domain and correcting unwrapped phase spectra for the phase delay due to propagation, we found source phases and SGTs for different source-station geometries. Fig. 1 demonstrates the similarity of the SGT obtained from the normal mode synthetics with results of calculations using the asymptotic formulas for the same combination of earth and source parameters, and the source–receiver geometries. The asymptotic description of SGT is accurate enough for our purposes in the whole period range, as the difference between the asymptotic and non-asymptotic SGT values is less than 2–3 s everywhere. Averaging results of similar

calculations for four different events and 10 stations provided the statistical support for this conclusion. The rms values of this difference change from 0.3 s at 40-s period to 2 s at 200-s period. This means that for an epicentral distance of 3000 km at period 100 s, the error in estimating group velocity using the asymptotic formalism is on the order of 0.15%, and for 6000 km on the order of 0.08%, which is at least one order of magnitude less than measurement errors (Ritzwoller and Levshin, 1998).

One should note that the stationary phase approach described in Appendix A (formulas A18–A21) is not valid at frequencies where the amplitude spectrum is changing rapidly (e.g., Pekeris, 1948), such as near nodes in the radiation pattern or near so-called ‘spectral holes’ where spectral amplitudes sharply decrease. Such changes are usually accompanied by a jump of π in phase. This means that the phase derivative with frequency does not exist locally. As a result, the numerical implementation of the asymptotic formalism can produce the physically unreasonable values of SGT near the π phase jumps. Such nonphysical values of SGT do not appear in measurements made on the normal mode synthetics due to averaging with frequency in the measuring procedure. The group times determined from the observed seismograms are also free from such physically unrealistic anomalies. This means that we need to be careful to exclude such singularities in the SGT corrections from consideration in our study.

3. Effects of source mechanism and depth on SGT delays of Rayleigh waves

As shown in Appendix A, SGT depends on several factors. For a given model of a laterally homogeneous or smooth laterally inhomogeneous medium, SGT is a function of the period T , the source depth h , the source mechanism (i.e., seismic moment tensor \mathbf{M}), and the source–receiver geometry; namely, the angle ψ between the strike of the fault and the direction from the epicenter to a station. Because the last factor varies widely from station-to-station and from event-to-event, we will consider the pattern of SGT for all possible values of ψ ($0^\circ \leq \psi < 360^\circ$) as a function of T and h . We will limit ourselves to consider only double-couple source mechanisms.

As an organizational device, we use a triangle of source mechanisms suggested by Kaverina et al. (1996). This condensed representation allows us to map all possible double-couple type mechanisms irrespective of the strike orientation, using the values of the plunges for their P , T , and N axes, into an area limited by an isosceles triangle (Fig. 2). Vertices N , T , and S (Fig. 2) of this triangle correspond, respectively, to a normal fault, a thrust fault along the 45° -dipping plane, and a pure strike-slip fault along a vertical plane. Bisectors divide this triangle into three parts according to the predominant type of mechanism, as labeled on Fig. 2. Selected types of mechanisms, whose positions inside the triangle are indicated by asterisks, are shown on the same figure. Because a change in the sign of the slip direction does not change the absolute value of the SGT, it is sufficient to consider mechanisms belonging to the left half of the triangle. To estimate how different source mechanisms are represented in world seismicity and in a subset of events used for the Eurasian surface wave tomography (Ritzwoller and Levshin, 1998), we show in Fig. 3 maps of the density of events inside the source triangle for several source depth intervals: 0–20, 20–40, 40–60, and 60–100 km from the CMT catalog and from the tomographic

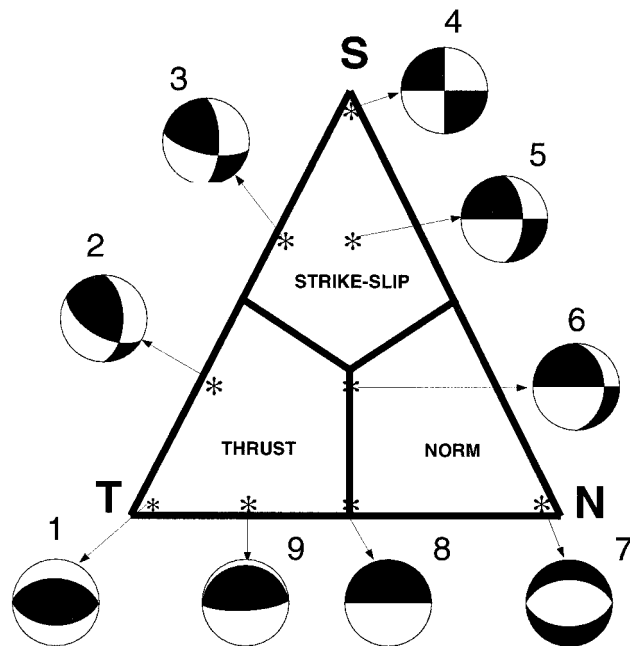


Fig. 2. Triangle representation of source mechanisms. Stars indicate positions of selected mechanisms inside the triangle (Kaverina et al., 1996). T , S , N denote thrust, strike-slip, and normal.

subset. Event density is defined in percentage as $N_c(x, y)/N_d^i$, where $N_c(x, y)$ is the number of events in a circle of fixed radius with a center at the point (x, y) inside the triangle, and N_d^i is (the number of events inside the i th depth interval) \times (the relative area of the circle). The size of the chosen circles and the number of events for each depth interval are shown in the figure. Both sets of diagrams show that for shallow source depths, strike-slip and normal events are as common as thrust events. When the source depth increases, the dominant type of mechanism is a thrust. Earthquakes with mechanisms in the central part of the triangle are rare. Before we start to analyze effects of source mechanisms on SGTs, we should note that mechanisms 1, 4, and 7 at the vertices of the triangle present extreme (degenerative) cases for which source phase does not change with frequency (except the jumps in π at the nodes of the radiation pattern). Consequently, the SGTs for these sources are zero independent of the azimuth of radiation. However, even in the near vicinity of these points inside of triangle we find significant non-zero SGT. Fig. 4a–c display normalized amplitude radiation patterns and patterns of the $SGT(\psi)$ for the fundamental Rayleigh wave in a slightly modified PREM model (Dziewonski and Anderson, 1981) in which the water layer is replaced by a layer of soft sediments. Each figure corresponds to one of three selected source mechanisms indicated by numbers 2, 3, and 9 in Fig. 2. The selection is based on the conclusions regarding the prevailing types of the source mechanisms among events with known CMT solutions and degeneracy at the vertices mentioned above. The associated focal mechanisms ('beachball' images) are shown at the top of each figure. The left column for each period–depth pair represents amplitudes normalized by the maximum value with azimuth, the middle column represents the SGT pattern (black filling is for positive values and grey filling is for negative values). The third column presents normalization information.

We observe a great diversity of SGT patterns for different periods, source depths and mechanisms. They are much more complex than amplitude radiation patterns for two main reasons. First, as mentioned earlier, the source phase may have a jump of π with period near the nodal planes of radiation. Second, the phase changes with period may be much

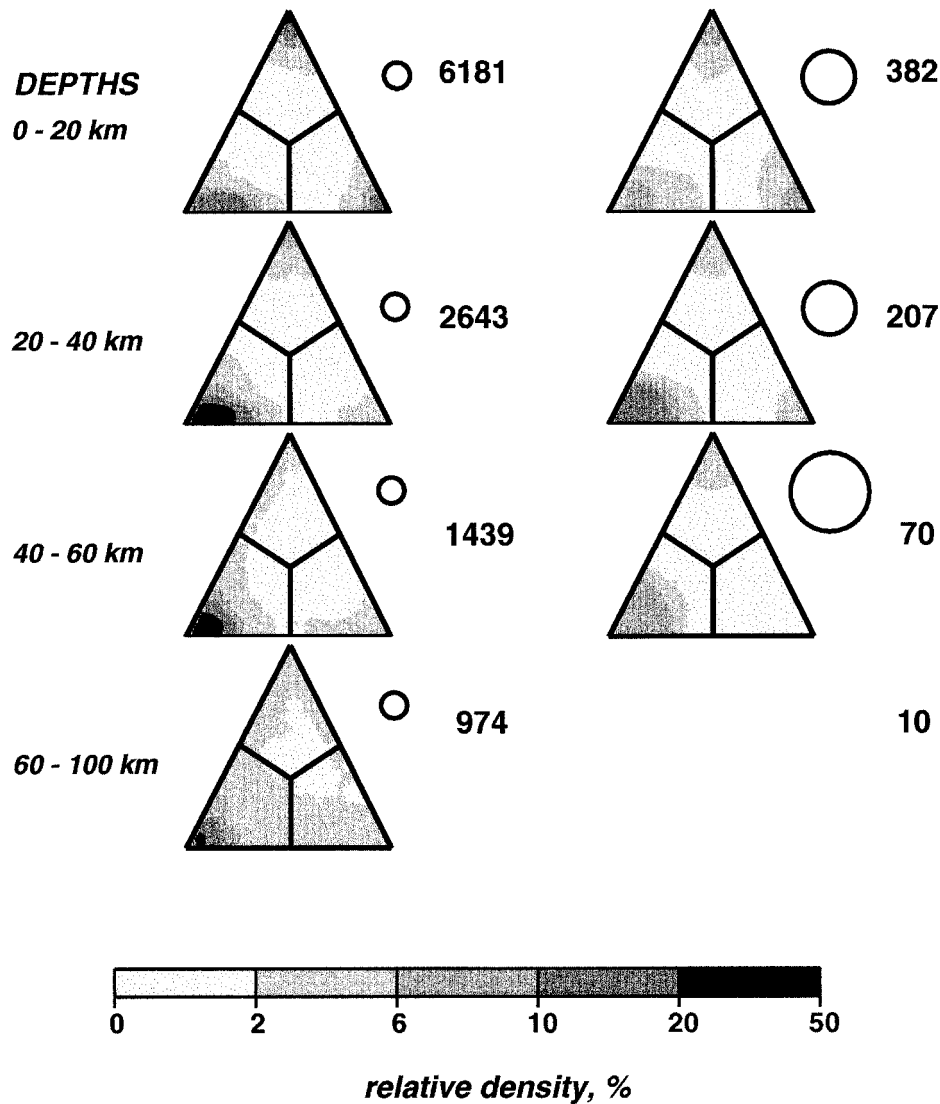


Fig. 3. Maps of the relative density of events inside the triangle for several source depth intervals. Two data sets are used: (1) all events from the Harvard CMT catalog for January 1977–November 1997; (2) events from the Eurasian surface wave tomography (Ritzwoller and Levshin, 1998). All source parameters are taken from the Harvard CMT catalog. Density is defined in percentage of $N_c(x, y)/N_d^i$, where $N_c(x, y)$ is the number of events in a circle of fixed radius with a center at the point (x, y) inside the triangle, and N_d^i is (the number of events inside the i th depth interval) \times (the relative area of the circle). The size of circles chosen and the number of events for each depth interval are shown. Thrust events are dominant for source depths more than 20 km in both data sets.

more rapid than the amplitude changes at some azimuthal directions.

A fault with a dominant vertical slip ('beachballs' 1, 7, 8, and 9 in Fig. 2) is characterized by zero or relatively small SGT values for practically all period–depth pairs. Strike-slip and thrust faults along inclined fault planes have the most significant SGT at periods above 75 s.

The average characteristics of SGT for different periods and source depths may be summarized in

different ways. We found the median values, \bar{S} , of the magnitude of the SGT as a function of azimuth ψ incremented by 1° to be a useful average. We mapped \bar{S} across the whole source triangle for a set of periods and depths. The resulting maps are shown in Fig. 5. For periods less than about 75 s, median values are less than 10 s for essentially all depths and source mechanisms and decrease with depth. For periods of 75 s and above, there are areas inside the source triangle with relatively high median values,

especially for strike-slip faults along inclined planes at depths greater than 50 km.

A more general conclusion about typical values of the magnitude of the SGT is obtained by finding and averaging median values \bar{S} for all events in the CMT catalog sorted by the depth into four source depth intervals, namely, 0–20, 20–40, 40–75, and 75–200 km. The resulting curves for the four source depth intervals are shown in Fig. 6. Very similar curves are obtained for events used for Eurasian tomography. The behavior of all four curves is similar. They are characterized at short periods by a rapid increase in average median value (AMV) with period, followed, after passing through a narrow inflection zone, by much slower changes. Shallow events (with source depths less than 20 km) are characterized by an AMV less than 5 s and the central period of the inflection zone at about 20 s. The AMV for events with source depths between 20 and 40 km is less than 12 s everywhere, grows rapidly with period, and stabilizes at a level of about 12 s at periods longer than 60 s. Events at depths between 40 and 75 km are characterized by an AMV below 10 s for periods below 75 s, rising to 20–25 s at periods above 100 s. For deeper events (75–100 km), the 10 s level of the AMV is reached at a period of about 140 s, and the 25 s level at 200-s period (the right end of period range considered.) Notice that events with depths greater than 40 km, which produce large SGT, are relatively rare in data sets which are normally used for fundamental mode group velocity measurements, such as events in the CMT catalog or the Eurasian tomography data set. This is illustrated by Fig. 7 which presents histograms of source depths for events from the CMT catalog and events used for group velocity tomography of Eurasia for source depths less than 200 km.

4. Distortions of tomographic images due to neglecting SGT

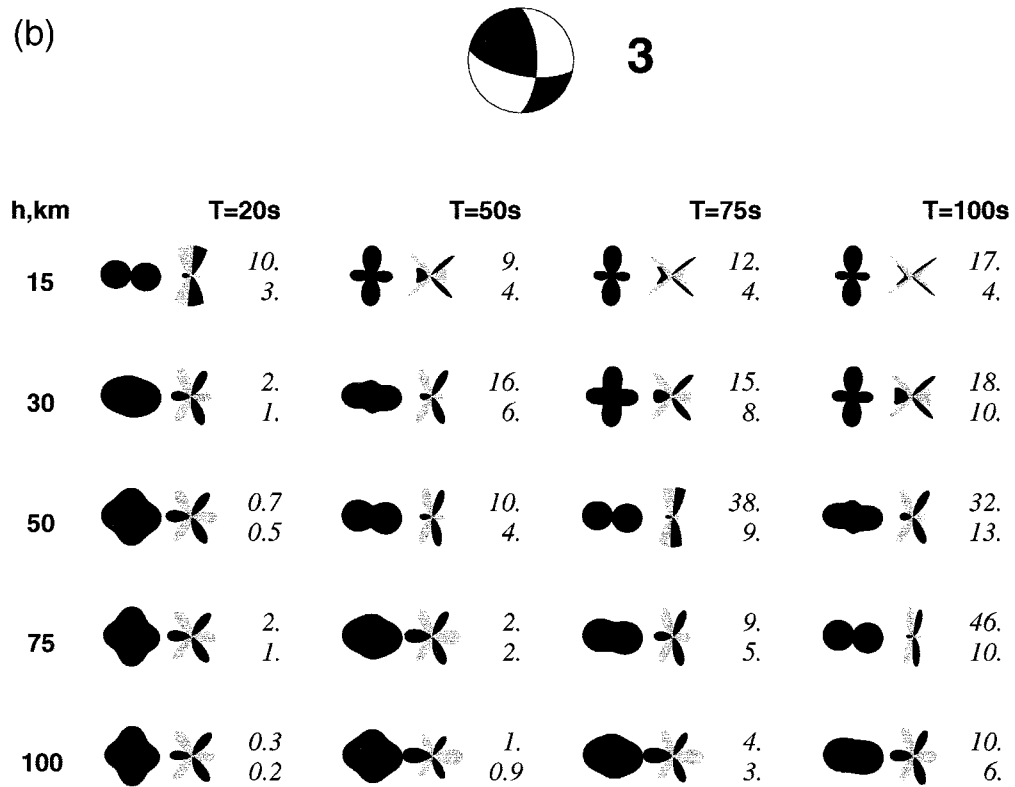
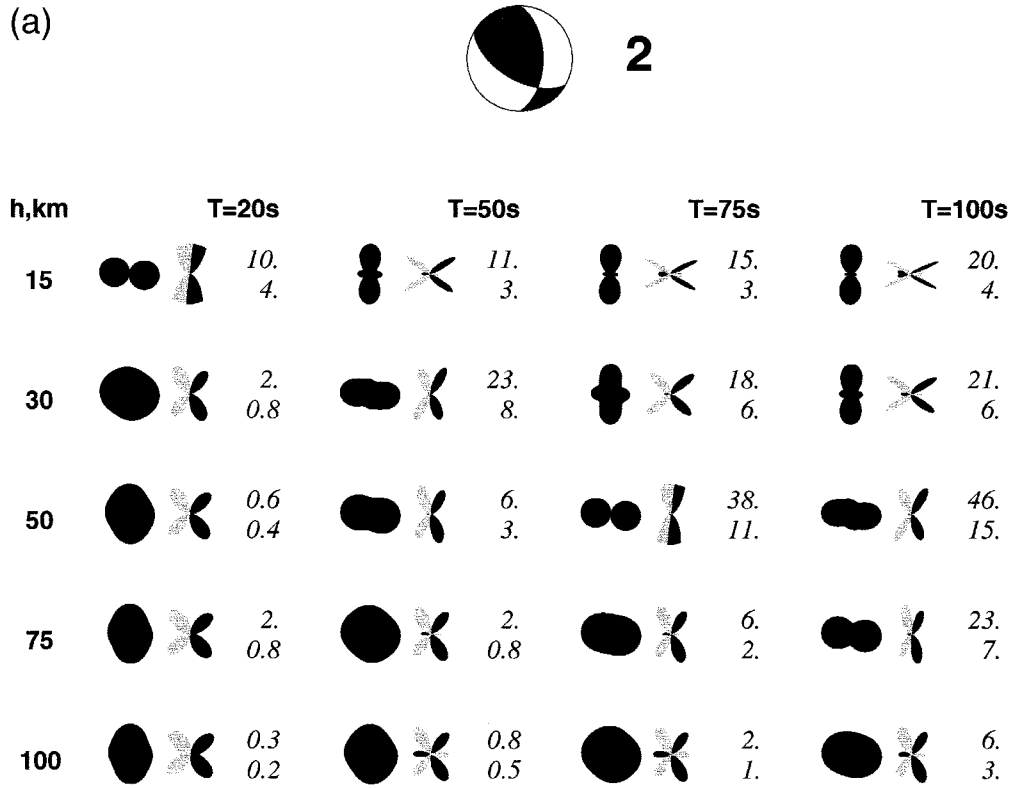
As we have shown in Section 3, SGT corrections are appreciable, especially at periods more than 75 s and for source depths more than 25 km. As they are usually neglected in tomographic studies, it is important to understand the level of bias produced in tomographic group velocity maps by neglecting SGT

corrections. We performed several synthetic tests to estimate this bias. In these tests, we used the same set of Rayleigh wave paths as in the tomographic inversion performed by Ritzwoller and Levshin (1998). Instead of the observed group velocity, we assigned to each ray the same fixed value of group velocity and then corrected it for the predicted group time shift. Thus, for the i th ray and the period T_j we have:

$$\mathcal{Z}_i(T_j) = \Delta_i / \left[\left(\Delta_i / \mathcal{Z}_r(T_j) \right) - S_i(T_j) \right],$$

where Δ_i is the length of the i th ray in km, and $\mathcal{Z}_r(T_j)$ is the fixed reference velocity.

As discussed in Section 2, the asymptotic formalism does not provide an accurate description of the wave field near nodes of source radiation patterns and inside of ‘spectral holes’. As a result, calculations based on asymptotic formulas (A22–A23) may predict for certain azimuths and periods unreasonably large and physically unjustified magnitudes of the SGT. To deal with this problem, we introduced some ad hoc but reasonable, empirical rules to identify and discard or reduce erroneous SGT corrections. These rules are based on using a parameter describing the distribution of magnitudes of SGT for a given source in the entire azimuth range, $0^\circ \leq \psi < 360^\circ$, to calibrate the predicted value for a given ray. We chose the median value, \bar{S} , of the magnitude of the SGT correction, $|\text{SGT}(\psi)|$, with ψ incremented by 1° to be this parameter. If the predicted magnitude of the SGT for a given ray and period is above some multiple of \bar{S} , the SGT correction is discarded and the observation is rejected. If the predicted magnitude of SGT is less than this limit but still above some smaller multiple of \bar{S} , the magnitude of SGT will be reduced to this smaller multiple but the sign of predicted SGT will be preserved. In formal terms these rules are: (1) the observation for the i th ray at period T_j is rejected if $|\text{SGT}_i(T_j)| \geq K_1 \bar{S}(T_j)$, (2) the magnitude of $\text{SGT}_i(T_j)$ is reduced to $K_2 \bar{S}(T_j)$ if $K_2 \bar{S}(T_j) < |\text{SGT}_i(T_j)| < K_1 \bar{S}(T_j)$. We chose coefficients K_1 and K_2 to equal, respectively, 5 and 3. The application of such rules to our data caused the rejection of 1–2% of the observations and a reduction in the SGT corrections to yield a change in the values of the group velocities for another 3–4% of all observations.



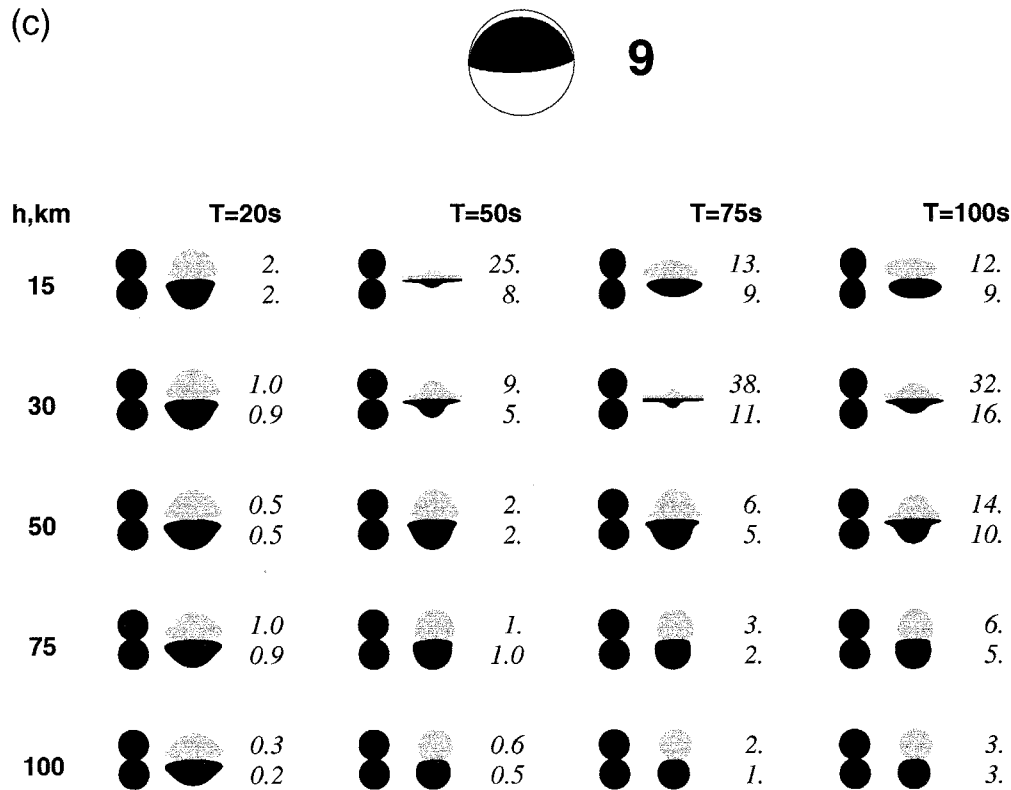


Fig. 4. (a) Amplitude radiation patterns and $SGT(\psi)$ diagrams of Rayleigh waves for source mechanism 2 shown on the top of the figure, at four different periods and five different source depths. Each element of the table comprises a trio of components for each depth–period pair. The left component is the amplitude pattern normalized by the maximum value for a given depth and period, the middle component is the SGT pattern (black filling is for positive values and grey filling is for negative values), and the right component is a set of two numbers related to the SGT diagram to their left. The upper number is the maximum plotted SGT value on the diagram (in s), and the lower number is the median value over azimuth in seconds of $|SGT(\psi)|$ sampled by 1° increments. The great variability of SGT radiation patterns with period and source depth is well seen. (b) Same as (a), but for source mechanism 3. (c) Same as (a), but for source mechanism 9.

Tomographic images for this synthetic input data set demonstrate the level of group velocity anomalies produced by uncorrected SGTs. Fig. 8a–c present such images for the Eurasian tomography Rayleigh wave data at periods 20, 50, and 100 s. The maximal anomalies for 20 s are of the order of 2.5%, for 50 s are less than 2%, and for 100 s are less than 5%. Significant anomalies dominantly are confined to the periphery of the maps (Western Pacific Arc, the Philippine Sea, Indochina). Even at 100-s period, anomalies across most of Eurasia are less than 1%. The maximum signal related to the lateral inhomogeneity of the crust and the upper mantle is on the order of 20% for 20–50 s period, and 5–8% for 100-s period (Ritzwoller and Levshin, 1998). This means that by neglecting SGT, we do not significantly distort the tomographic images, except in marginal areas at long periods. This is understand-

able because SGT corrections vary in sign and magnitude from one seismic zone to another, and their effect averages nearly to zero for internal regions crossed by many differently oriented paths. Only for the rim of Eurasia, where most of paths begin or terminate, and the number of crossing paths is very small, are the effects of uncorrected SGT relatively important. This is especially true at long periods.

5. Sensitivity of SGT corrections to source characteristics

As shown at Section 3, the magnitude of SGT can easily be above 10–15 s for periods above 75 s and source depths larger than 25 km. This means that some of observed group velocities uncorrected for SGT may be appreciably distorted. At the same time,

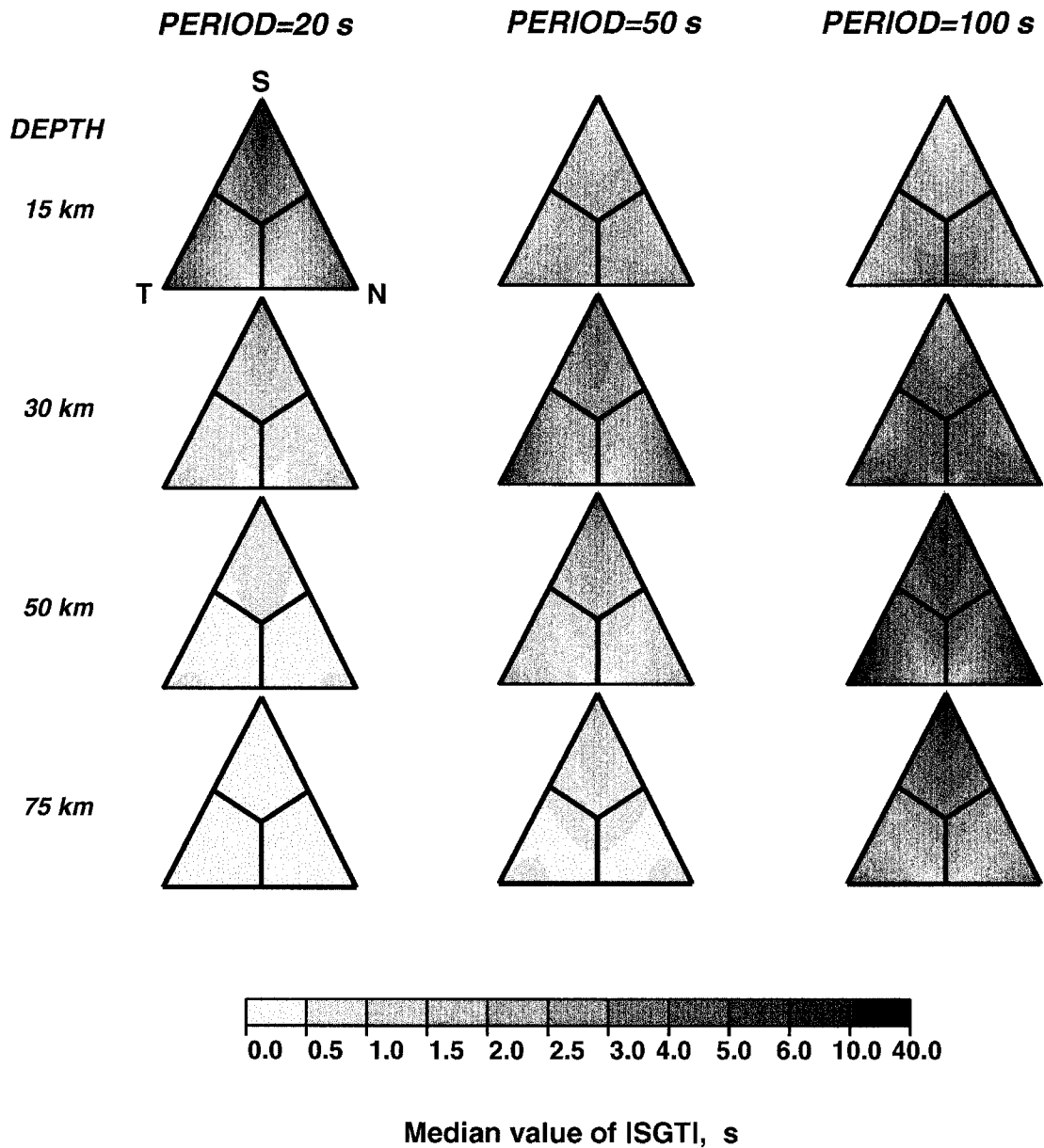


Fig. 5. Maps of median values, \bar{S} , of $|\text{SGT}(\psi)|$ across the source triangle for periods 20, 50, and 100 s. Median values for periods 20 and 50 s are below 12 s and decrease as the source depth increases. For the 100-s period, median values are above 10 s for a significant part of the source triangle and increase with depth.

the tomographic experiment based on the Eurasian tomographic data set discussed in Section 4 demonstrated the existence of appreciable bias due to uncorrected SGT at the rim of the continent. These results imply that it may be advisable to apply SGT corrections in group velocity studies.

To evaluate the practical importance of applying SGT corrections we consider data obtained from adjacent ray paths (Ritzwoller and Levshin, 1998).

Measurements whose path endpoints lie within 2% of the path length are grouped to produce a 'cluster' of dispersion curves. Averaging the curves composing the cluster provides an average cluster dispersion curve. To exemplify the effects of uncorrected SGT on group velocity measurements, we selected several clusters of seismic events and several recording stations. For each event and station, we compared group velocity curves obtained with and without

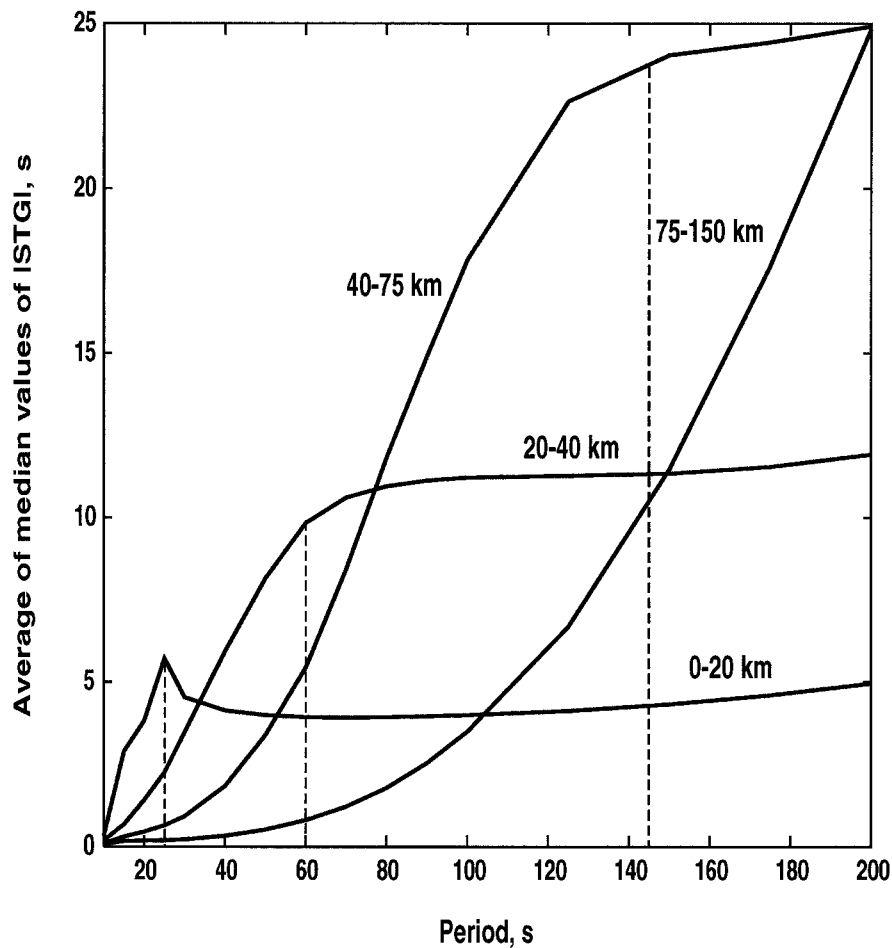


Fig. 6. Averages of median values of $|\text{SGT}(\psi)|$ for events at different depth intervals (all events from the Harvard CMT catalog for January 1977–November 1997). The dashed lines divide parts of curves with different dependence on period: fast growth with increasing period to the left of the dashed line, and slow changes to the right of this line.

corrections for SGT. As an example, we show in Fig. 9 the rms values of group velocity deviations relative to the average values for two station-event pairs: Eastern Iran to Arti, Russia (ARU), and Kuril Islands to Obninsk, Russia (OBN). In the first case, the cluster consists of four events, and in the second case, 16 events. In the first case, SGT corrections increase the rms difference between the measured group velocities in the cluster across wide range of periods. Evidently, introducing SGT corrections increases the level of noise in our data for this cluster of events. In the second case, the introduction of the corrections slightly decreases the rms differences.

More general estimates may be obtained if we average similar results for all clusters present in our Rayleigh wave data for Eurasia. The number of such

clusters is quite large (e.g., around 4500 at 40-s period). We compared the average rms deviations between individual group velocities and their cluster averages for corrected and uncorrected data and found the differences between the average rms for all clusters to be very small; namely, less than 0.005 km/s for the entire range of periods. Such small differences are statistically insignificant, being evidently much less than measurement errors and observational errors due to the inaccuracy in the spatial and temporal locations of earthquakes provided by the CMT catalog and measurement errors (Ritzwoller and Levshin, 1998). In addition, there is no systematic decrease of the average rms deviations when SGT corrections are introduced for subsets of data with different ranges of source depths.

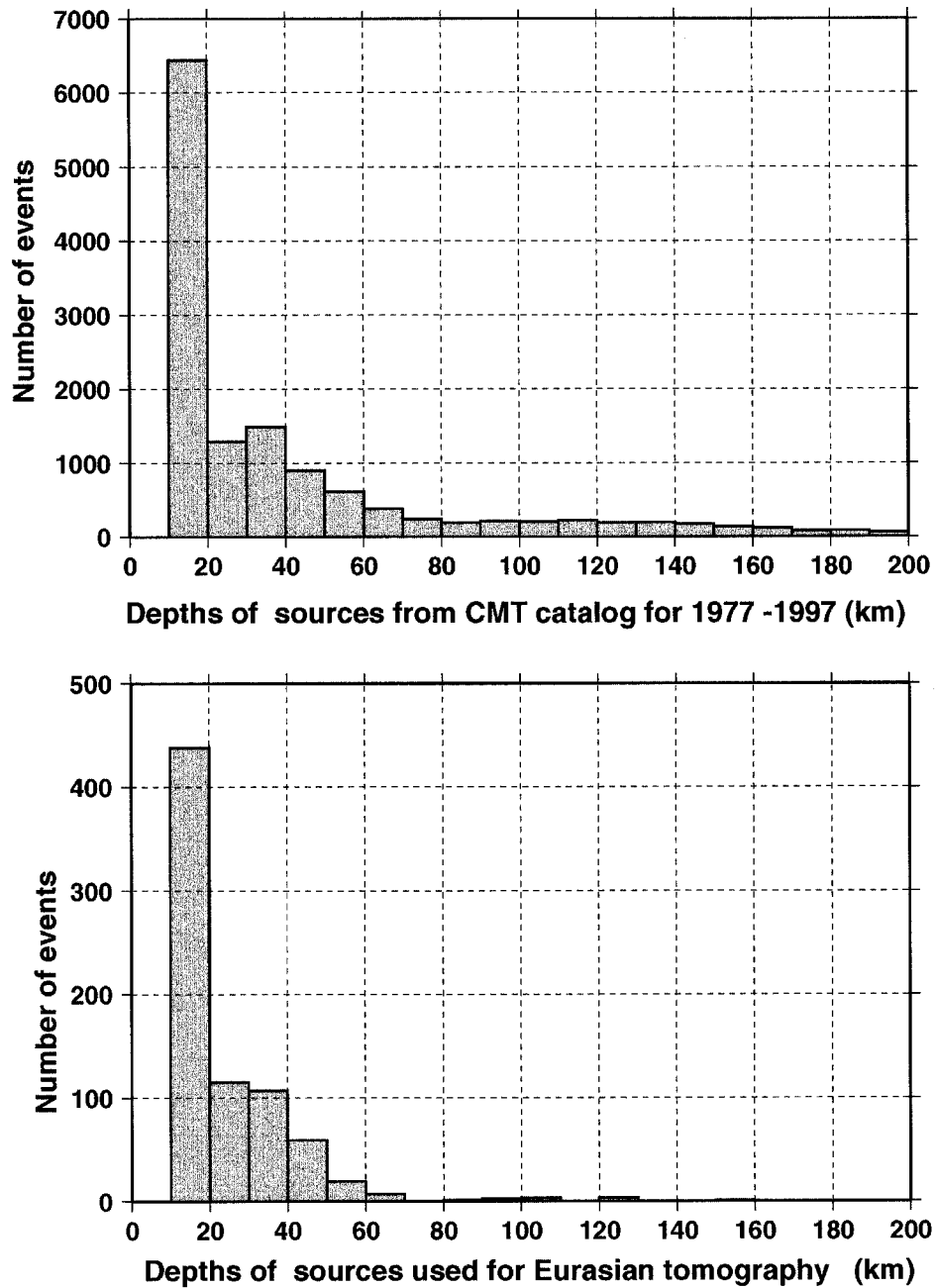
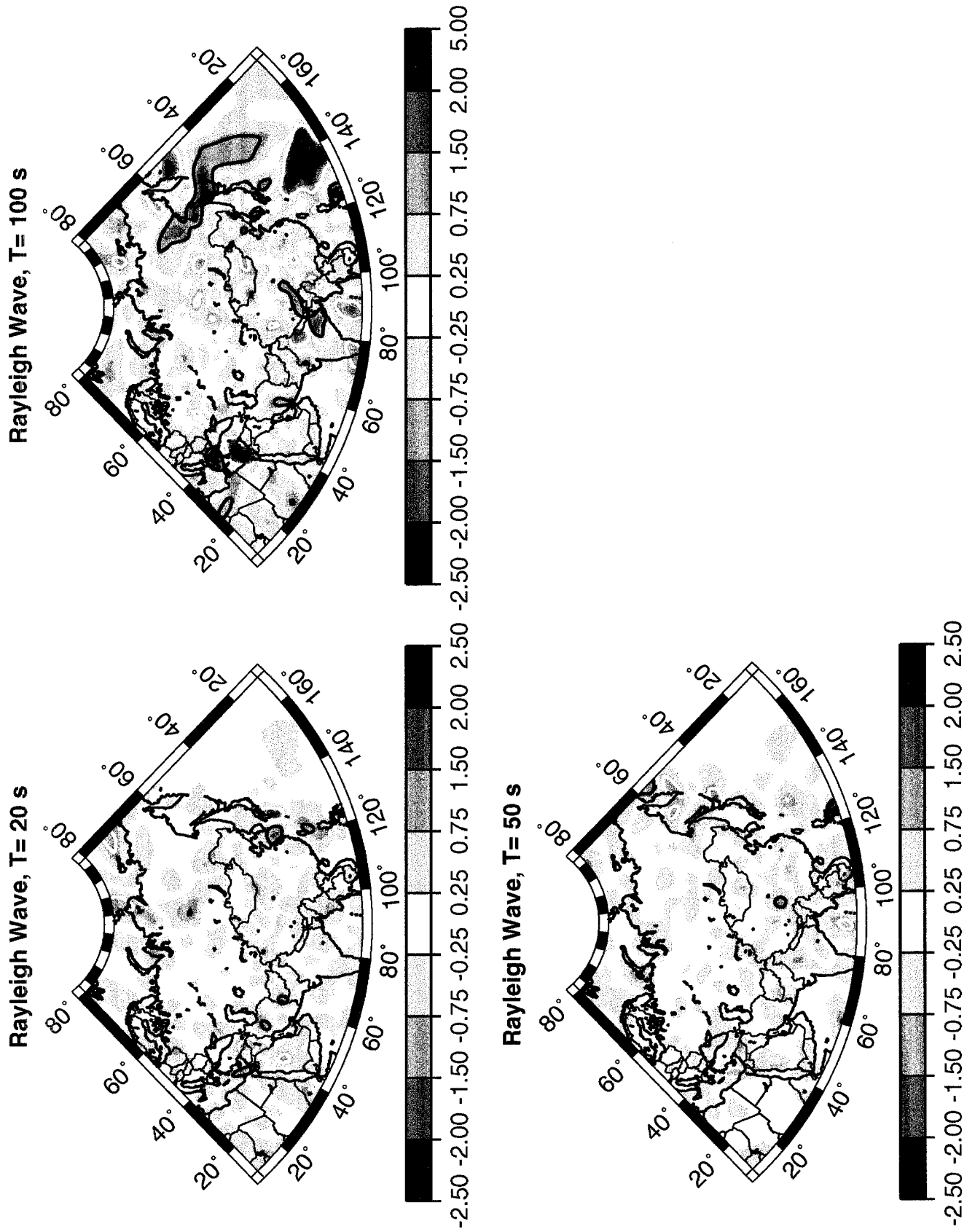


Fig. 7. Histograms of source depths in the depth interval 0–200 km: (top) for all events from the Harvard CMT catalog from January 1977 to November 1997 (bottom) for events used for Eurasian surface wave tomography (Ritzwoller and Levshin, 1998). The fraction of events with depths greater than 40 km used in surface wave tomographic studies is much smaller than in the CMT catalog.

The absence of improvements in group velocity cluster rms statistics after introducing SGT correc-

tions requires explanation. We estimated the sensitivity of possible SGT corrections to random errors in

Fig. 8. Bias produced by neglecting SGT shift in Eurasian tomographic studies (Ritzwoller and Levshin, 1998). Estimated bias for the 20, 50 and 100 s Rayleigh waves is expressed as the percentage error relative to the average group velocity across the region of study for each period. The $\pm 1\%$ contours are drawn (black, +; white, -). Significant bias (above 1% of the reference velocity) appears predominantly near the rim of the continent at long periods.



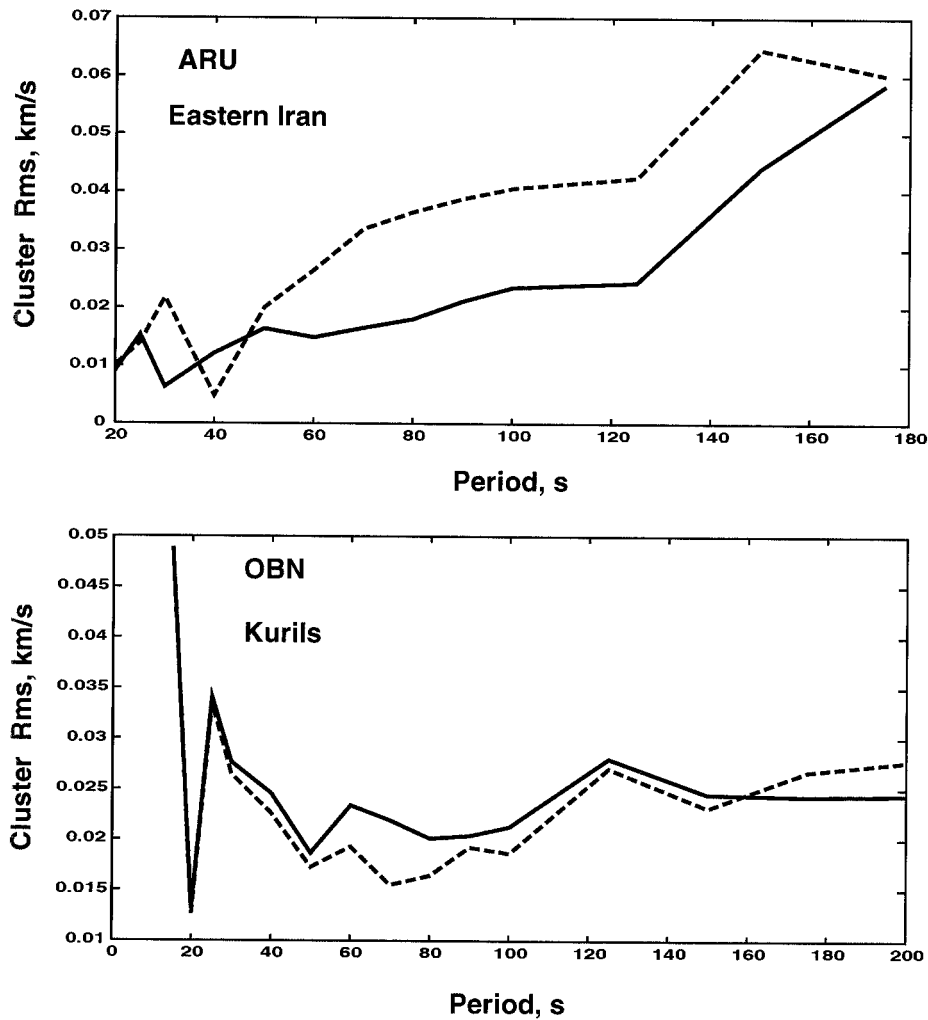


Fig. 9. Comparison of rms group velocity deviations from the average Rayleigh wave group velocity curve for two clusters of measurements. (Top) Events in Eastern Iran recorded at the station ARU (Arti, Russia). (Bottom) Events near the Kuril Islands recorded at the station OBN (Obninsk, Russia). Solid lines are for group velocity measurements without SGT corrections applied, and dashed lines are obtained after corrections. No significant decrease in rms due to corrections for SGT is observed.

source depth and source mechanism. Muzyert and Snieder (1996) took a similar approach for SPT corrections. Fig. 10a and b demonstrate the magnitude of changes of SGT for two earthquakes from the CMT catalog: on 10/18/1996 in Japan with centroid depth of 22 km (top), and on 1/01/1996 in the Philippines with a centroid depth of 33 km (bottom) for a fixed azimuth (135°) far from the nodal direction of the Rayleigh wave radiation pattern for both events. Fig. 10a shows changes in SGT(T) when the depth of the source is changed by ± 10 km. The radiation pattern for 50 s and the azimuthal direction for which the SGT(T) is presented are shown in the upper left corner of each

subfigure, and the source mechanisms are shown in the upper right corners. It is evident from this figure that a realistic uncertainty on the order of 10 km in the source depth may produce an effect comparable in size to the magnitude of the SGT correction itself. Fig. 10b shows the effect of 20% changes in the values of the components of the moment tensor for these two events (the zero trace of the moment tensor is preserved). In this case, the effect on the SGT is less significant, especially for the second event. Similar numerical experiments with other events lead us to conclude that SGT is strongly sensitive to errors in depth and only weakly sensitive to errors in the moment tensor. It should be remem-

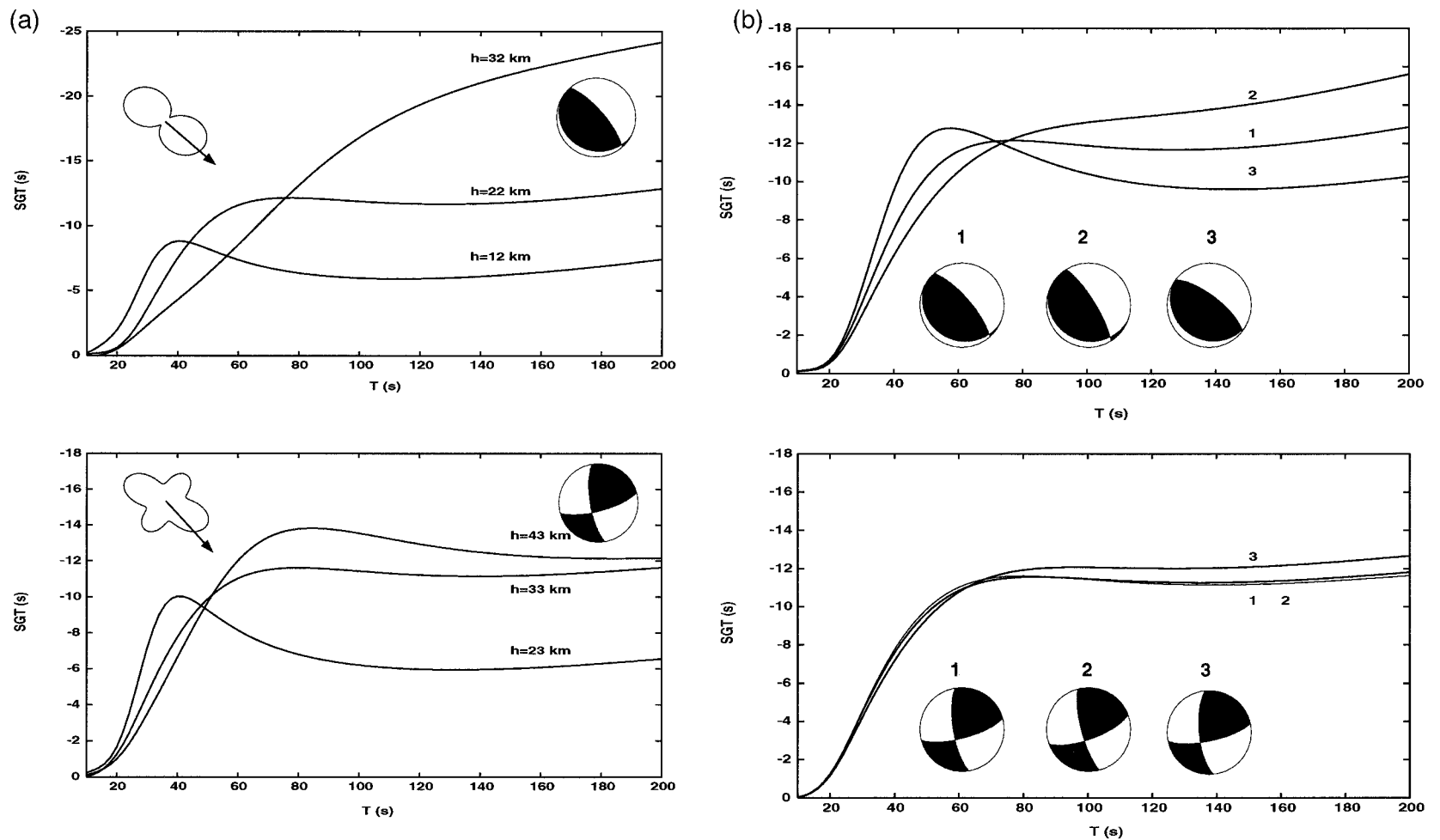


Fig. 10. The effects of errors in source depth and moment tensor on SGT for different periods. Two earthquakes are selected from the CMT catalog: (top) on 10/18/1996, 1026 h at Japan with a centroid depth of 22 km, and (bottom) on 1/01/1996, 2242 h at the Philippines with a centroid depth of 33 km for a fixed azimuth (135°). (a) Changes in $SGT(T)$ when the depth of the source is changed by ± 10 km. The radiation pattern for 50 s and azimuthal direction for which $SGT(T)$ is presented are shown at the upper left corner of each subfigure. The source mechanisms are shown at the upper right corners. Significant changes of SGT values due to errors in source depth are seen. (b) Changes in $SGT(T)$ when values of moment tensor components are changed by 20%. Corresponding variations of the source mechanism are shown. Changes of SGT values caused by perturbations of the moment tensor are relatively small.

bered that this problem is exacerbated by the fact that for many seismic events, the data used for finding the CMT solution do not provide adequate depth resolution, and the source centroid depth in the CMT catalog is fixed at 15 km.

It is evident from our experiments that deviations of the real source depth from the CMT value by ± 5 –10 km probably produce errors in the SGT that vitiate the corrections. Unless source depth is very well-known, then, the efficacy of the SGT corrections is compromised and a positive effect of the application of the corrections is far from guaranteed.

6. Conclusions

In this study, we estimated the possible effect of SGT on group velocity measurements for fundamental Rayleigh waves generated by double-couple type seismic events. We have studied the dependence of this effect on period (10–100 s), source mechanism, and depth (15–100 km). We found that there is a great variability in azimuthal patterns and magnitude of SGT depending on these three factors. Statistics of certain salient functionals that characterize the dependence of SGT on different factors were presented, e.g., the median values of SGT magnitude as a function of azimuth from epicenter to station for different periods, source depths and mechanisms.

The main conclusions of our study are as follows.

(1) SGT corrections are generally small and may be neglected in group velocity measurement for periods less than 75 s and source depths less than 25 km. For longer periods and especially for deeper events, SGT corrections are appreciable.

(2) The perturbations produced by uncorrected SGT in tomographic inversions of Rayleigh wave group velocity data for the Eurasian continent are generally very small (less than 1% of the unperturbed values), but appreciable perturbations (up to 1–2% for the 50-s period and up to 5% for the 100-s period) are found near the edge of the continent where ray coverage is poor.

(3) SGT corrections are very sensitive to errors in the source depth. If extremely accurate depth determination are available the SGT corrections should be applied at periods above 75 s, especially for events

deeper than 25 km. However, taking into account the accuracy of most CMT solutions for earthquake depth and the magnitude of observational errors in measuring group velocities, at present, SGT corrections are practically non-essential for group velocity tomographic studies.

Acknowledgements

We thank Michel Cara, an anonymous reviewer, and Barbara Romanowicz (Ed.) for critical comments on this paper which substantially improved its content. We are very grateful to Alexander Lander for his help in the triangular representation of source mechanisms. This work was supported by the US National Science Foundation Grants NSF-OPP-9615139 and NSF-EAR-9706188, and the US Department of Defense Contract DSWA01-97-C-0157.

Appendix A. Surface wave formalism

A.1. Laterally homogeneous medium

First, consider surface wave propagation in a laterally homogeneous isotropic elastic half-space. We use a source-centered cylindrical coordinate system (r, φ, z) , $0 \leq r < \infty$, $0 \leq \varphi < 2\pi$, $0 \leq z < \infty$. Let a point source situated at the point $(0, 0, h)$ be described by the seismic moment tensor $\mathbf{M}H(t)$, where t is time, H is the step function, and \mathbf{M} is a symmetrical second-order tensor. The receiver is at the point $(r, \varphi, 0)$ on the free surface. The 1D model is characterized by a piece-wise continuous vector-function $\mathbf{m}(z)$, $\mathbf{m} = (\alpha, \beta, \rho)$, where α and β are P - and S -velocities and ρ is density. We assume that there exists a depth Z at which α and β reach their maximum values and are constant at depths $z \geq Z$. The displacement observed at the receiver is:

$$\mathbf{d}(t, r, \varphi, h) = \frac{1}{2\pi} \int_{-\infty}^{\infty} \mathbf{D}(\omega, r, \varphi, h) \exp(i\omega t) d\omega, \quad (\text{A1})$$

where r is the epicentral distance, ϕ the epicentral azimuth, and h is the source depth. The displace-

ment spectrum is the sum of body waves, leaking modes, and normal modes or surface waves:

$$\mathbf{D} = \mathbf{D}_B + \mathbf{D}_L + \mathbf{D}_S. \quad (\text{A2})$$

The surface wave spectrum may be further decomposed into fundamental and overtone modes depending on the radial order n of the mode, $\mathbf{D}_S = \sum_n \mathbf{D}_S^{(n)}$, where the fundamental surface wave has $n = 0$. Hereinafter, we set $n = 0$ and suppress the index n . Let \mathbf{e}_r , \mathbf{e}_φ , \mathbf{e}_z be the local unit vectors at the receiver, so $\mathbf{D}_S = D_r \mathbf{e}_r + D_\varphi \mathbf{e}_\varphi + D_z \mathbf{e}_z$, where the φ -direction is transverse to the great-circle linking source to receiver and the r -direction is radially outward from the source along the great-circle. Love waves are confined to the φ -component of the seismogram and Rayleigh waves are found on the r - and z -components. We, therefore, set $D_\varphi = D_L$, $D_r = D_{Rr}$, and $D_z = D_{Rz}$ where R represents Rayleigh waves and L represents Love waves. With these definitions, it is well-known (Aki and Richards, 1980; Levshin et al., 1989) that the complex displacement spectrum of the fundamental surface waves may be asymptotically presented as:

$$\begin{aligned} D_L(\omega, r, \varphi, h) &= \frac{\exp(-i\pi/4)}{\omega\sqrt{8\pi r}} \frac{\exp(-ik_L(\omega)r)}{\sqrt{k_L(\omega)} \mathcal{E}_L(\omega) \mathcal{Z}_L(\omega) I_L(\omega)} \\ &\quad \times \mathcal{S}_L(\omega, r, \varphi, h), \end{aligned} \quad (\text{A3})$$

$$\begin{aligned} D_{Rz}(\omega, r, \varphi, h) &= \frac{\exp(-i3\pi/4)}{\omega\sqrt{8\pi r}} \frac{\exp(-ik_R(\omega)r)}{\sqrt{k_R(\omega)} \mathcal{E}_R(\omega) \mathcal{Z}_R(\omega) I_R(\omega)} \\ &\quad \times \mathcal{S}_R(\omega, r, \varphi, h) \end{aligned} \quad (\text{A4})$$

$$\begin{aligned} D_{Rr}(\omega, r, \varphi, h) &= \exp(-i\pi/2) \\ &\quad \times D_{Rz}(\omega, r, \varphi, h) \epsilon(\omega), \end{aligned} \quad (\text{A5})$$

if

$$k_L r \gg 2\pi, k_R r \gg 2\pi, r \gg h. \quad (\text{A6})$$

Here $k_L(\omega)$ and $k_R(\omega)$ are horizontal wavenumbers, $\mathcal{E}_R(\omega) = \omega/k_r$ and $\mathcal{E}_L(\omega) = \omega/k_L$ are phase velocities, $\mathcal{Z}_R(\omega) = (dk_R/d\omega)^{-1}$ and $\mathcal{Z}_L(\omega) = (dk_L/d\omega)^{-1}$ are group velocities, and $\epsilon(\omega)$ is a real

ellipticity factor. The integrals I_R and I_L are normalization integrals proportional to the kinetic energies of the corresponding waves \mathcal{S}_R and \mathcal{S}_L are the source-excitation functions defined below.

Let $U(\omega, z)$ and $V(\omega, z)$ be the 1D Rayleigh wave vertical and horizontal eigenfunctions of model \mathbf{m} , respectively, and let $W(\omega, z)$ be the 1D Love wave eigenfunction. With these definitions the normalization integrals are:

$$I_R(\omega) = \int_0^\infty \rho(z) [U^2(\omega, z) + V^2(\omega, z)] dz, \quad (\text{A7})$$

$$I_L(\omega) = \int_0^\infty \rho(z) W^2(\omega, z) dz, \quad (\text{A8})$$

and the Rayleigh and Love wave source-excitation functions can be written as:

$$\begin{aligned} \mathcal{S}_R &= U'(\omega, h) M_{zz} + k_R(\omega) V(\omega, h) \\ &\quad \times [M_{xx} \cos^2 \varphi + M_{xy} \sin 2\varphi + M_{yy} \sin^2 \varphi] \\ &\quad - iV'(\omega, h) [M_{xz} \cos \varphi + M_{yz} \sin \varphi] \\ &\quad + ik_R(\omega) U(\omega, h) [M_{xz} \cos \varphi + M_{yz} \sin \varphi], \end{aligned} \quad (\text{A9})$$

$$\begin{aligned} \mathcal{S}_L &= k_L(\omega) W(\omega, h) [M_{xx} \sin \varphi \cos \varphi \\ &\quad - M_{xy} \cos 2\varphi - M_{yy} \sin \varphi \cos \varphi] \\ &\quad - iW'(\omega, h) [M_{xz} \sin \varphi - M_{yz} \cos \varphi], \end{aligned} \quad (\text{A10})$$

where, for example, $U'(\omega, h)$ denotes the value of $dU(\omega, z)/dz$ evaluated at $z = h$.

It is seen from formulas (A3)–(A10) that the components of the complex displacement spectrum may be presented as:

$$D_L = |D_L(\omega, r, \varphi, h)| \exp[i\Psi_L(\omega, r, \varphi, h)], \quad (\text{A11})$$

$$D_{Rz} = |D_{Rz}(\omega, r, \varphi, h)| \exp[i\Psi_R(\omega, r, \varphi, h)], \quad (\text{A12})$$

$$\begin{aligned} D_{Rr} &= |D_{Rr}(\omega, r, \varphi, h)| \epsilon(\omega) \exp[i\Psi_R(\omega, r, \varphi, h) \\ &\quad - (\pi/2)], \end{aligned} \quad (\text{A13})$$

where the phase spectrum is:

$$\Psi_L = -k_L(\omega)r - \pi/4 + \psi_L^S(\omega, \varphi, h), \quad (\text{A14})$$

$$\Psi_R = -k_R(\omega)r - 3\pi/4 + \psi_R^S(\omega, \varphi, h). \quad (\text{A15})$$

The source phases, ψ_L^S and ψ_R^S , are correspondingly

$$\psi_L^S = \tan^{-1} [Im(\mathcal{S}_L)/Re(\mathcal{S}_L)], \quad (\text{A16})$$

$$\psi_R^S = \tan^{-1} [Im(\mathcal{S}_R)/Re(\mathcal{S}_R)], \quad (\text{A17})$$

which are seen to be functions of frequency, source depth, and source–receiver geometry. Both functions are model-dependent because they depend on the ratio between the real and imaginary terms on right side of Eqs. (A9) and (A10) which include the model eigenfunctions and their first depth derivatives.

Group velocities derive from the application of the stationary phase approximation in converting the displacement spectrum into time-domain seismograms (e.g., Pekeris, 1948; Aki and Richards, 1980; Levshin et al., 1989). Following this approach, the observed group arrival times, $t_{\mathcal{Z}_R}(\omega)$ and $t_{\mathcal{Z}_L}(\omega)$, of the Rayleigh and Love waves at frequency ω follow from the frequency derivative of the phase spectrum:

$$0 = \frac{d(\omega t_{\mathcal{Z}_R} + \Psi_R)}{d\omega} \rightarrow t_{\mathcal{Z}_R} = \frac{r}{\mathcal{Z}_R(\omega)} - \frac{d\psi_R^S}{d\omega}, \quad (\text{A18})$$

$$0 = \frac{d(\omega t_{\mathcal{Z}_L} + \Psi_L)}{d\omega} \rightarrow t_{\mathcal{Z}_L} = \frac{r}{\mathcal{Z}_L(\omega)} - \frac{d\psi_L^S}{d\omega}. \quad (\text{A19})$$

The observed group velocities are:

$$\mathcal{Z}_R^{\text{obs}}(\omega) = \frac{r}{t_{\mathcal{Z}_R}(\omega)} = r \left[\frac{r}{\mathcal{Z}_R(\omega)} - T_R(\omega) \right]^{-1}, \quad (\text{A20})$$

$$\mathcal{Z}_L^{\text{obs}}(\omega) = \frac{r}{t_{\mathcal{Z}_L}(\omega)} = r \left[\frac{r}{\mathcal{Z}_L(\omega)} - T_L(\omega) \right]^{-1}, \quad (\text{A21})$$

where we have defined the SGT, T_R and T_L , of the Rayleigh and Love waves as that part of the ob-

served group arrival time that comes from the source phase:

$$T_L(\omega, r, \varphi, h) = \frac{d\psi_L^S}{d\omega}, \quad (\text{A22})$$

$$T_R(\omega, r, \varphi, h) = \frac{d\psi_R^S}{d\omega}. \quad (\text{A23})$$

A.2. Smoothly laterally inhomogeneous medium

When the model \mathbf{m} is a function of the horizontal coordinates r and φ , but changes in the elastic parameters, density, and boundary topography are relatively smooth, the formulas above can be generalized in the ray approximation (e.g., Woodhouse, 1974; Babich and Chikhachev, 1975; Babich et al., 1976; Levshin, 1985; Levshin et al., 1989; Tromp and Dahlen, 1992). According to this asymptotic theory, functions characterizing surface waves, such as \mathcal{E}_R , \mathcal{Z}_R , k_R , U , V , I_R , ϵ for Rayleigh waves, and \mathcal{E}_L , \mathcal{Z}_L , k_L , W , I_L for Love waves, are defined by the local one-dimensional model corresponding to the structure under a given point at the free surface (r, φ) . As a result, these functions become dependent on the horizontal coordinates (r, φ) . Surface waves propagate along ray tubes whose geometry is defined by the scalar fields $\mathcal{E}_L(\omega, r, \varphi)$, $\mathcal{E}_R(\omega, r, \varphi)$, respectively.

This approach leads to the following expressions for the Rayleigh and Love wave phase spectra (Levshin, 1985; Levshin et al., 1989):

$$\Psi_R = -\omega \int_S \frac{ds}{\mathcal{E}_R(\omega, s)} - 3\pi/4 + \psi_R^S(\omega, \phi_R(\omega, r, \varphi), h - z_0(0,0)), \quad (\text{A24})$$

$$\Psi_L = -\omega \int_S \frac{ds}{\mathcal{E}_L(\omega, s)} - \pi/4 + \psi_L^S(\omega, \phi_L(\omega, r, \varphi), h - z_0(0,0)), \quad (\text{A25})$$

where ψ_L^S and ψ_R^S are defined in Eqs. (A16) and (A17). SGTs are found as in the spherical case by differentiating ψ_L^S and ψ_R^S by ω . The main difference here is that the emergence angle from the source for the ray that arrives at the receiver, ϕ_R or ϕ_L , may differ somewhat from the azimuth of the great-circle between source and receiver due to lateral refractions of rays caused by inhomogeneities in the medium of propagation.

References

- Aki, K., Richards, P.G., 1980. *Quantitative Seismology: Theory and Methods*, Vol. I. Freeman, San Francisco.
- Babich, V.M., Chikhachev, B.A., 1975. Propagation of Love and Rayleigh waves in weakly inhomogeneous media. *Vestnik LGU* 1, 32–38.
- Babich, V.M., Chikhachev, B.A., Yanovskaya, T.B., 1976. Surface waves in a vertically inhomogeneous half-space with weak horizontal inhomogeneity. *Izv. AN SSSR, Fiz. Zemli (Solid Earth)* 4, 24–31.
- Calcagnile, G., D'Ingeo, F., Farruga, P., Panza, G.F., 1982. The lithosphere in the Central–Eastern Mediterranean area. *Pure Appl. Geophys.* 120, 389–406.
- Cara, M., 1973. Filtering of dispersed wave trains. *Geophys. J. R. Astron. Soc.* 33, 65–80.
- Cara, M., Hatzfeld, D., 1976. Vitesse de groupe de l'Onde de Rayleigh de part et d'autre de la ligne Açores-Gibraltar. *Ann. Geophys.* 32, 85–91.
- Curtis, A., Woodhouse, J., 1997. Crust and upper mantle shear velocity structure beneath the Tibetan plateau and surrounding regions from interevent surface wave phase velocity inversion. *J. Geophys. Res.* 102, 11789–11813.
- Dziewonski, A.M., Anderson, D.L., 1981. Preliminary reference earth model. *Phys. Earth Planet. Inter.* 25, 297–356.
- Dziewonski, A.M., Bloch, S., Landisman, M., 1969. A technique for the analysis of transient seismic signals. *Bull. Seismol. Soc. Am.* 59, 427–444.
- Dziewonski, A.M., Chou, T.-A., Woodhouse, J.H., 1981. Determination of earthquake source parameters from waveform data for studies of global and regional seismicity. *J. Geophys. Res.* 86, 2825–2852.
- Ekström, G., Tromp, J., Larson, E.W.F., 1997. Measurements and global models of surface wave propagation. *J. Geophys. Res.* 102, 8147–8158.
- Gilbert, F., 1976. The representation of seismic displacements in terms of travelling waves. *Geophys. J. R. Astron. Soc.* 44, 275–280.
- Gilbert, F., Dziewonski, A.M., 1975. An application of normal mode theory to the retrieval of structural parameters and source mechanisms from seismic spectra. *Philos. Trans. R. Soc. London, Ser. A* 278, 187–269.
- Jimenez, E., Cara, M., Rouland, D., 1989. Focal mechanisms of moderate earthquakes from the analysis of single-station three-component surface-wave records. *Bull. Seismol. Soc. Am.* 79, 955–972.
- Kaverina, A.N., Lander, A.V., Prozorov, A.G., 1996. Global creepex distribution and its relation to earthquake-source geometry and tectonic origin. *Geophys. J. Int.* 125, 249–255.
- Knopoff, L., 1972. Observation and inversion of surface wave dispersion. *Tectonophysics* 13, 497–519.
- Knopoff, L., Schwab, F.A., 1968. Apparent initial phase of a source of Rayleigh waves. *J. Geophys. Res.* 73, 755–760.
- Landisman, M., Dziewonski, A.M., Sato, Y., 1969. Recent improvements in the analysis of surface wave observations. *Geophys. J. R. Astron. Soc.* 17, 369–403.
- Laske, G., Masters, G., 1996. Constraints on global phase velocity maps from long-period polarization data. *J. Geophys. Res.* 101, 16059–16075.
- Levshin, A.L., 1985. Effects of lateral inhomogeneities on surface wave amplitude measurements. *Ann. Geophys.* 3 (4), 511–518.
- Levshin, A.L., Pisarenko, V.F., Pogrebinsky, G.A., 1972. On a frequency–time analysis of oscillations. *Ann. Geophys.* 28, 211–218.
- Levshin, A.L., Yanovskaya, T.B., Lander, A.V., Bukchin, B.G., Barmin, M.P., Ratnikova, L.I., E.N., 1989. In: Keilis-Borok, V.I. (Ed.), *Its Seismic Surface Waves in a Laterally Inhomogeneous Earth*. Kluwer Publ., Dordrecht.
- Levshin, A.L., Ratnikova, L., Berger, J., 1992. Peculiarities of surface wave propagation across Central Eurasia. *Bull. Seismol. Soc. Am.* 82, 2464–2493.
- Muyzert, E., Snieder, R., 1996. The influence of errors in source parameters on phase velocity measurements of surface waves. *Bull. Seismol. Soc. Am.* 86, 1863–1872.
- Nolet, G., 1987. Waveform tomography. In: Nolet, G., Reidel, D. (Eds.), *Seismic Tomography with Applications in Global Seismology and Exploration Geophysics*. Norwell, MA, pp. 301–322.
- Panza, G.F., Schwab, F.A., Knopoff, L., 1973. Multimode surface waves for selected focal mechanisms: I. Dip-slip sources on a vertical fault plane. *Geophys. J. R. Astron. Soc.* 34, 265–278.
- Pekeris, C.L., 1948. Theory of propagation of explosive sound in shallow water. *Geological Society of America Memoirs*, No. 27.
- Ritzwoller, M.H., Levshin, A.L., 1998. Eurasian surface wave tomography: group velocities. *J. Geophys. Res.* 103, 4839–4868.
- Ritzwoller, M.H., Levshin, A.L., Smith, S.S., Lee, C.S., 1995. Making accurate continental broadband surface wave measurements. In: Lewkowicz, J.F., McPhetres, J.M., Reiter, D.T. (Eds.), *Proceedings of the 17th Seismic Research Symposium on Monitoring a CTBT, Phillips Lab., Hanscom AFB, MA*, pp. 482–490.
- Ritzwoller, M.H., Levshin, A.L., Ratnikova, L.I., Egorin, A.A., 1998. Intermediate period group velocity maps across Central Asia, western China, and parts of the Middle East. *Geophys. J. Int.* 134, 315–328.
- Russell, D.W., Herrman, R.B., Hwang, H., 1988. Application of frequency-variable filters to surface wave amplitude analysis. *Bull. Seismol. Soc. Am.* 78, 339–354.
- Snieder, R., 1988. Large-scale waveform inversion of surface waves for lateral heterogeneity: 2. Application to surface wave in Europe and Mediterranean. *J. Geophys. Res.* 93, 12067–12080.
- Stevens, J.L., Day, S.M., 1985. The physical basis of m_b , M_s and variable frequency magnitude methods for earthquake/explosion discrimination. *J. Geophys. Res.* 90, 3009–3020.
- Trampert, J., Woodhouse, J., 1995. Global phase velocity maps of Love and Rayleigh waves between 40 and 150 seconds. *Geophys. J. Int.* 122, 675–690.
- Tromp, J., Dahlen, F.A., 1992. Variational principles for surface wave propagation on a laterally heterogeneous Earth, I, II. *Geophys. J. Int.* 109, pp. 581–598 and 599–619.

- Vdovin, O.Y., Rial, J.A., Ritzwoller, M.H., Levshin, A.L., 1999. South American surface wave tomography: group velocities. *Geophys. J. Int.*, in press.
- Woodhouse, J.H., 1974. Surface waves in the laterally varying layered structure. *Geophys. J. R. Astron. Soc.* 37, 461–490.
- Woodhouse, J.H., Dziewonski, A.M., 1984. Mapping the upper mantle: three-dimensional modeling of Earth structure by inversion of seismic waveforms. *J. Geophys. Res.* 89, 5953–5986.
- Wu, F.T., Levshin, A., 1994. Surface wave tomography of China using surface waves at CDSN. *Phys. Earth Planet. Inter.* 84, 59–77.
- Wu, F.T., Levshin, A.L., Kozhevnikov, V.M., 1997. Rayleigh wave group velocity tomography of Siberia, China and the vicinity. *Pure Appl. Geophys.* 149, 447–473.
- Zhang, Y.S., Tanimoto, T., 1993. High-resolution global upper mantle structure and plate tectonics. *J. Geophys. Res.* 98, 9793–9823.